ChemPubSoc Europe

DOI: 10.1002/cphc.201601143

CHEMPHYSCHEM Articles

Special Issue

Effects of Water Intercalation and Tribochemistry on MoS_2 Lubricity: An Ab Initio Molecular Dynamics Investigation

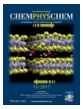

Giacomo Levita*[b] and Maria C. Righi*[a, b]

To date, no clear conclusion has been reached on the atomistic mechanisms that govern the observed decrease of lubricating capabilities of MoS_2 in humid environments. Based on ab initio molecular dynamic calculations, we show that intercalated water molecules hinder the sliding motion of both regular and defective layers considerably, with the velocities decaying exponentially with time. However, in the presence of an applied load and exposed edge terminations, water is rapidly removed from the interface and is adsorbed on the edges either in undissociated form or as OH/H fragments. These outcomes suggest that the interlayer slipperiness can be reduced by the presence of water even in the absence of any chemical oxidation. Our work could help to set up more dedicated experiments to further tackle a technologically relevant issue for the applications of MoS_2-based lubricants.

1. Introduction

MoS_2 is one of the most important solid lubricants, with applications ranging from aerospace to automotive industries, thanks to its ultralow friction coefficient[1–6] and low toxicity.[7,8] However, the advantages of MoS_2 use are lost in humid atmosphere where its friction coefficient increases markedly.[9–15] Despite experimental advances that have led to a greater understanding of the fundamental mechanisms behind the water–MoS_2 interaction,[16–23] to date no clear explanation on how water negatively affects its lubricating properties has been provided.

Scientific literature is discordant on this point. On the one hand, some authors stress the importance of chemical oxidation of MoS_2 layers, which leads to the formation of MoO_3, which has worse frictional characteristics than MoS_2:[12,24–26] such a process has been reported to be activated by water vapour.[9] On the other hand, some point to the lack of oxidation evidenced in humid, but anaerobic environments[27] and suggest that molecular interactions of water with the MoS_2 layers is the fundamental mechanism behind the observed loss of lubricant properties.[20,28] No recent theoretical work has been reported on such a fundamental issue: previous works seemed to support the oxidation path,[6] but an atomistic study describing the origin of the increased friction of MoS_2 in humid atmosphere at the atomic scale is still required. This is striking when considering the increasing number of applications of MoS_2 and the increasing number of theoretical studies on its other unique electronic and magnetic properties.[29–37]

Recently, we carried out a static investigation of the interaction of water with MoS_2 based on density functional (DFT) calculations.[22] We found that water physisorbs on MoS_2 monolayers but its adsorption as an intercalated molecule inside a bilayer is unfavoured with respect to external adsorption. Moreover, no major changes are evidenced in the presence of S-atom vacancies on the layer as water adsorbs without any dissociation, pointing to the lack of oxidation taking place on basal planes even when defected. It is at the edges (both armchair and zigzag) where water is strongly adsorbed and where dissociation into H and OH may take place.[18,38] However, reconstructions reduce the edge reactivities markedly and thereby their capacity to bind water molecules.[18,22,39]

Having carried out the static study, a subsequent step requires a dynamic investigation on both the physical and the chemical interactions between water molecules and MoS_2 layers. In the first case we consider water intercalation, because from the tribologic point of view one might expect that the increase of interlayer distance caused by intercalated molecules could lead to an improvement of the frictional properties of MoS_2 bilayers. We therefore carried out ab initio molecular dynamics simulations of sliding layers with intercalated water molecules, analysing their behaviour upon load and shear application to highlight why, under these conditions, humidity is found to actually hinder the sliding properties. As a following step, because of the adoption of the ab initio MD approach, which allows chemical processes occurring at the sliding interface to be accurately described,[40] we could monitor whether oxidation processes at the edges can be activated by water dissociation assisted by mechanical stresses. In other words,

[a] Prof. M. C. Righi
Dipartimento di Scienze Fisiche, Informatiche e Matematiche
Universitá di Modena e Reggio Emilia
I-41125 Modena (Italy)
E-mail: mcrighi@unimore.it

[b] Dr. G. Levita, Prof. M. C. Righi
Istituto Nanoscienze, CNR—Consiglio Nazionale delle Ricerche
I-41125 Modena (Italy)
E-mail: glevita@units.it

Supporting Information for this article can be found under: https://doi.org/10.1002/cphc.201601143.

An invited contribution to a Special Issue on Mechanochemistry

we can address fundamental questions regarding the role of water in modifying frictional mechanisms in MoS_2.

2. Systems and Methods

The study was carried out based on ab initio molecular dynamics calculations performed with the Car–Parrinello (CP) method,[41] making use of an in-house modified version of the plane-wave and pseudopotential computer code included in the QuantumEspresso package.[42] The adopted modifications allow the relative motion of contacting surfaces to be simulated. The modified version of the CP computer code has been successfully used to describe the tribochemical reactions of diamond interfaces interacting with water.[40,43]

To model extended MoS_2 layers we used periodically repeated (4×4) hexagonal supercells, the short and long diagonals being, respectively, 12.79 and 22.16 Å. To model finite 2D ribbons, a rectangular supercell measuring 11.08 Å×19.19 Å was used instead, allowing about 10 Å of free space between periodic images along the *y* direction. Armchair-terminated edges (extending on the *x* direction) were considered, because they have slightly higher formation energy than the zigzag forms and the largest reactivity towards water:[22] therefore they should be most prone to oxidative processes. Moreover, in contrast to zigzag terminations,[38,44,45] they are not magnetic, thereby simplifying the calculations.

To model van der Waals interactions, the semi-empirical Grimme scheme[46,47] was used to correct the GGA-based Perdew–Burke–Ernzerhof parametrization[48,49] of the exchange-correlation functional (PBE-D); such a set-up had proved to correctly reproduce key geometric parameters of many layered structures including MoS_2.[31,50–52] The *k*-points sampling was limited to the Gamma point. The energy cut-off for the plane-wave expansion was set to 40 Ry, following the static DFT set-up;[22,51] a Methfessel–Paxton smearing[53] of 0.01 Ry was employed to take into account possible metallization along the edges.

The simulations were carried out under high load and temperature, which, at the microscopic level, help to accelerate tribochemical reactions: we chose a working temperature of 320 K and a 11 GPa applied contact pressure. As MoS_2 basal planes extend on the *xy* plane of the supercell, a uniaxial normal stress was mimicked by applying equal and opposite forces on the upper and lower layer along the *z* direction. The sliding motion was modelled by means of equal and opposite forces along the longer supercell diagonal, to which we henceforth associate the *y* direction. The simulated time intervals ranged between 7 and 10 ps for the extended layers systems (in particular 7 ps for 25% and 50% water coverages, 8 ps for 0% coverage; 10 ps for the S-vacancy system). The simulations including edge terminations lasted about 5 ps. In all the simulations the lateral forces were applied during the first 3 ps: after force removal, the systems were subsequently allowed to evolve without any shear stress applied.

In the course of the dynamics, we assigned the electrons a fictitious mass of 450 a.u.; the equations of motions were integrated with the Verlet algorithm with a time step of 0.12 fs. To avoid any unwanted coupling between the ionic and electronic degrees of freedom, deuterium was used instead of hydrogen. The temperature of the system was gradually increased before starting the actual dynamics, and then kept constant by means of a double chain of Nose–Hoover thermostats with frequencies 30 THz and 15 THz. An additional Nose–Hoover thermostat was applied on the electronic degrees of freedom with frequency 200 THz. To avoid the thermostat influencing the sliding motion imposed by the lateral forces, we specifically modified the version of the code[40] to subtract the velocity of the centre of mass from the atomic velocities considered within the thermostat.

The starting geometry for the infinite bilayers with a 25% intercalated water coverage was obtained by replicating four times the minimum energy configuration of a 2×2 supercell with an intercalated water molecule, as was obtained by static DFT calculations.[22] To model the 50% coverage, we inserted four additional molecules in the resulting 4×4 supercell, keeping the relative water–water distance as large as possible. The molecules were then allowed to change their arrangement upon thermal and shear motion without constraints. For all simulations, the initial interlayer distance was set to the equilibrium distance for the specific load and lateral configuration as obtained by DFT calculations.

3. Results and Discussion

We carried out two sets of dynamical studies. In the first, we considered extended periodic layers—with and without defects—to investigate the effect of water intercalation. In the second, we considered ribbons with active edges to check their tendency to attract water, and to monitor any kind of oxidative reaction. By combining these outcomes, a clear picture emerges on the atomistic mechanisms taking place at humid MoS_2 interfaces and on their tribologic consequences.

To study the effects of water physically interacting with the MoS_2 layers, we first compared the sliding behaviour of bilayers under load presenting a 0%, 25% and 50% coverage of intercalated water. In all cases we applied a shear stress lasting approximately 3 ps, then we allowed the system to evolve without any lateral force applied. Figure 1 reports the distance d(*t*) covered by the upper layer with respect to the lower layer as a function of time after the removal of the lateral forces (black curves).

It is interesting to note that d(*t*) varies with time as in the motion of a body under the effect of a viscous force. Indeed the red dashed curves of Figure 1 represent the expression $d(t)=(v_0/B)(1-e^{-Bt})$, which is the solution of the equation of motion in the presence of a force with a linear dependence on the velocity, $\mathbf{f} \propto -v(t)$. The (v_0/B) term, where v_0 is the sliding velocity at the moment of force removal and *B* is a numerical parameter proportional to the friction coefficient, represents the asymptotic distance d_∞ of the layers in the presence of a viscous friction.

Table 1 reports the d_∞ and *B* parameters obtained by fitting the simulation data for each coverage. By analysing Figure 1 and Table 1 it can be seen that 3.0 picoseconds after the force

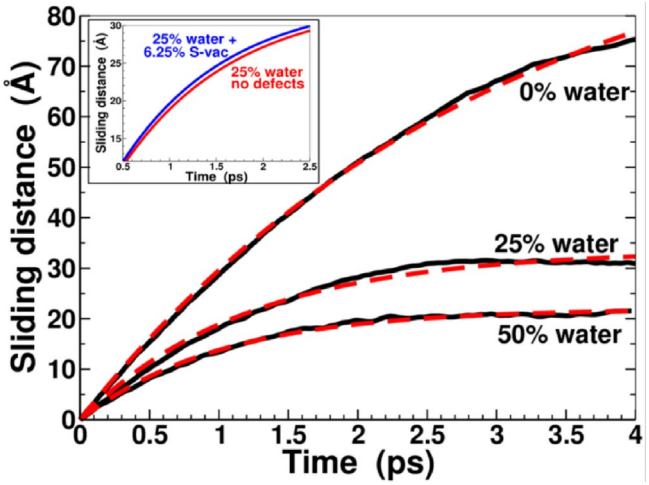

Figure 1. Comparison of the in-plane distances covered by MoS_2 bilayers after removal of the lateral force at different water coverages (black lines). The red dashed curves are obtained by fitting the data as described in the main text. Inset: the distance covered by a bilayer with no defects (red line) is compared to a S-vacant layer (blue line) at 25% water coverage.

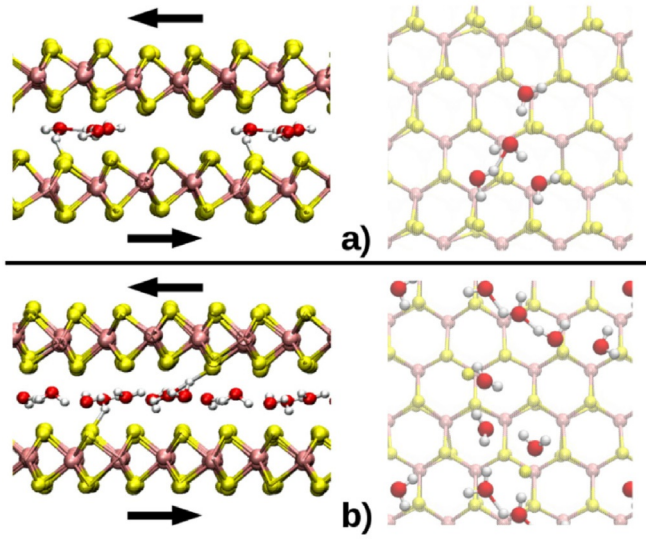

Figure 2. Snapshots from the dynamic trajectory of the 25% coverage (a) and 50% coverage (b) systems under load and shear. Typical water molecule networks are represented from side (left) and top (right) views.

Table 1. Fitted values of the asymptotic distance, d_∞, and the inverse of the characteristic time, B, in the exponential expression of the sliding distance for the viscous layer motion.

Coverage [%]	d_∞ [Å]	B [ps^{-1}]
0	104.4	0.33
25	33.5	0.83
50	22.0	0.99

removal, the layers containing the larger amount of intercalated water (50%) had spanned a distance of $0.95d_\infty$; at the same time, the values for the 25% interfacial coverage was $0.92d_\infty$ and at 0% coverage the bilayer was still shearing, having spanned just $d = 0.63d_\infty$. Whereas the absolute values of these asymptotic distances depend on the initial velocity, the percentages just described do not, and their values show that larger amounts of intercalated water induce a quicker stoppage after removal of the external shear. The $1/B$ parameter therefore expresses the characteristic time for the exponential decay of the velocity. The monotonic increase of B from 0 to 50% coverage points to the larger retardant effect of water on the sliding motion.

By inspection of the full atomic trajectories, no chemical reactions were observed in any of the dynamics involving infinite bilayers (movies for the 25 and 50% coverage are included in the the Supporting Information as Movie 1 and 2, respectively). It is just the physical water–layer interactions that slow down the shear motion. From the snapshots of Figure 2, corresponding to configurations frequently encountered by visual inspection during the course of the dynamics, we observe that water molecules show a marked tendency towards interacting with each other through H-bonds. At low coverage, such as the 25% case (Figure 2a), the molecules typically form trimers or tetramers, which leave some areas of the interface free from intercalation. At higher coverage, such as at 50% (Figure 2b), the network of interacting water molecules can extend further across the sliding interface. Although we did not carry out a clustering analysis on the occurrence of such configurations, their high frequency rate is revealed by a simple visual inspection of the trajectories in the movies. We also note that in the 25% system the formation of small water clusters induces a slight curvature in the bilayer, because water-free zones have lower interlayer distance than the intercalated area.

The formation of water clusters is related to the formation of strong hydrogen bonds, which, in the absence of layer defects, help prevent the centre of mass of the water molecules from drifting between the two MoS_2 layers moving in opposite directions. However, despite the low tendency of MoS_2 basal planes to chemically interact with intercalated water, the strong van der Waals interactions between MoS_2 and H_2O[20,54] render water a jamming, retardant layer that hinders the sliding motion instead of helping it.

A head-to-head comparison between a regular MoS_2 layer and one presenting a single S-atom vacancy (the most stable defect on a MoS_2 layer)[55–57] allows us to check whether basal plane defects chemically interact with intercalated water, for example catalysing its dissociation, and how they modify the sliding properties. Chemical reactions may also be accelerated by the perpendicular applied load, as previously observed in other systems.[40,43] The presence of defects in the system was simulated by introducing a S-vacancy density of 6.25% on the lower MoS_2 layer, with the upper layer left unchanged. In both cases, we chose a 25% water coverage, corresponding to four water molecules per supercell.

In the case of systems with no defects, the water molecules moved randomly around their initial positions without modifying their centre of mass; in contrast, in the S-vacant case, one water molecule is adsorbed on the vacancy as soon as the sliding reduces the vacancy–water distance below 4 Å. At this stage the molecule follows the lower layer along its motion:

such configuration is retained throughout the whole extension of the dynamics, during which a second water molecule regularly interacts with the adsorbed molecule through a H-bond. However, the adsorbed H_2O never dissociates into OH and H, which is consistent with earlier DFT findings[19,22] predicting an energy cost of 0.59 eV for the H/OH case with respect to the adsorption of an isolated H_2O molecule.

Figure 3a shows three snapshots selected from the whole trajectory (reported in the Supporting Information as Movie 3),

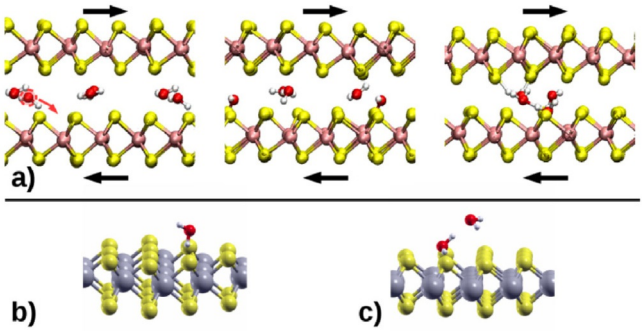

Figure 3. a) Snapshots from the dynamic trajectory of the S-vacant system under load and shear: the water molecule marked by a red circle is driven towards the vacancy, located where the red arrows points, then it is physisorbed either individually or as a (short-lived) trimer. Equilibrium geometries for b) one and c) two water molecules physisorbed on a S-vacant layer. Structures in panels (b) and (c) were determined by means of static DFT calculations.

in which we highlight the initial drift of water towards the vacancy, then the physisorption of one molecule and finally the coordination of an intercalated trimer formed through H-bonds. The latter configurations (again selected by visual inspection among the many similar ones occurring in the course of the trajectory) reflect those of minimum energy obtained from static calculations at 0 K for the adsorption of, respectively, one and two water molecules (Figures 3b,c). The net effect of the S-vacancy is therefore to attract and bind water molecules, removing them from the centre of the interface without promoting oxidative adsorption for at least 10 ps after the start of the simulation.

By plotting the sliding trajectory of the S-defective case, we found that the curve is almost coincident with that of the undefected 25% coverage (as evidenced by the comparison reported in the inset of Figure 1). This indicates that the interlayer sliding motion is not significantly affected by the presence of the vacancies. Furthermore we observed that isolated S atom vacancies do not induce modifications on the interlayer water film coverage or composition.

To further investigate the behaviour of water at the MoS_2 interface, we carried out dynamic simulations in which the bilayer presents edges. The presence of open terminations allows water to escape from the interlayer region. As a first step, we replaced the upper infinite layer with a 2D ribbon, as reported in Figure 4, and the shear stress was applied perpendicular to its termination. The latter was chosen as the regular armchair edge, because this proved to be the most reactive towards ad-

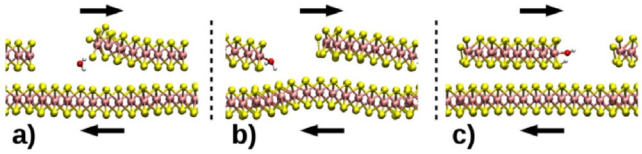

Figure 4. Snapshots from the dynamic trajectory of the system composed by one ribbon on an extended layer (periodic boundary conditions are applied along the lateral direction): a) a water molecule is escaping from the interfacial region (on the other side the interlayer distance is reduced by the applied load along *z*); b) water is attached to the ribbon edge; c) the planar bilayer configuration is restored and the sliding proceeds more smoothly.

sorption of molecular water.[22,45] We chose a very low water coverage (6.5%) to avoid any contribution from H-bonds with other molecules and we again applied a 11 GPa load.

Figure 4 evidences how, despite this high load, the upper ribbon is opened up from its initial geometry (even before application of the lateral shear) by the water molecule trying to escape the interface to reach the exposed edge (see Movie 4 in the Supporting Information for the whole trajectory).

We note the formation of an S–S dimer reconstruction along the lifted edge: such a reconstruction has already been reported in theoretical papers,[18,25,39,44] and reduces the edge energy. Water is therefore more strongly attracted by the unreconstructed edge on the adjacent ribbon, where it is absorbed on the exposed Mo atom, in agreement with the optimised geometry (shown in Figure 5a) obtained in our static DFT calcula-

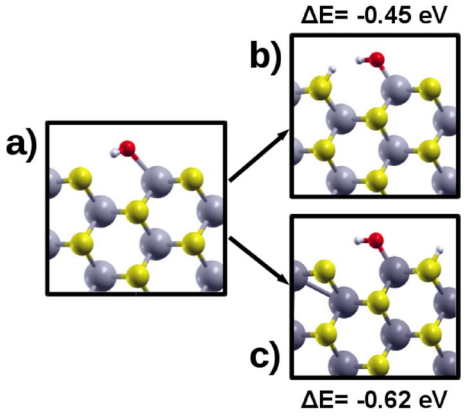

Figure 5. Adsorption configuration for a water molecule on the armchair edge (an H atom is eclipsed by the other H atom), (a). Dissociative configurations presenting the two water fragments on opposite sides of an edge trench (b) or on the same MoS_2 unit (c).

tions.[22] The molecular adsorption in this configuration is associated with an energy gain of 1.34 eV;[22] in the course of the dynamics, after a few femtoseconds, H_2O dissociates into H and OH (Figure 5b), which produces an energy gain of 0.45 eV with respect to molecular adsorption. This geometry is formed more easily from the adsorbed H_2O than the configuration shown in Figure 5c, which is slightly more stable but requires a hydrogen transfer to a more distant sulfur atom.[22]

A corrugation of the lower layer is also observed, following the inclination of the upper ribbon: upon shear application,

the bilayer—after water is eliminated from the interface and after edge reconstruction—recovers its planar structure with the interlayer distance corresponding to that expected from DFT calculations for a 11 GPa load and starts sliding exactly as in the anhydrous case discussed earlier. In other words, the sliding becomes effective after a water-free interface is formed between parallel MoS_2 layers.

To establish whether the tendency of the interface to expel water is valid also at higher water content, we increased the coverage to 25% and replaced the lower MoS_2 layer with a ribbon with the same width as the upper layer, as reported in Figure 6a (the full movie can be found in the Supporting Information as Movie 5). One water molecule per cell, placed outside the interface, is immediately attached to a Mo atom of the upper ribbon edge as observed in the previous case. Moreover, also here the left side of the ribbon lifts (Figure 6b) to expel from the interface two water molecules per supercell: these molecules rapidly reach the upper and lower edges of the ribbons. As we apply both a load perpendicular to the interface and a shear parallel to it, the ribbons are induced to rotate: given the presence of active edges that are only partially saturated with water coming from the interface, the layers collide and start interconnecting (Figure 6c) although a full layer reconstruction is inhibited by water adsorbed on the damaged edge terminations.

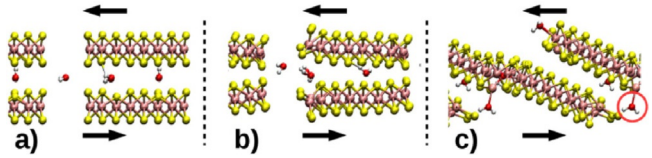

Figure 6. a) The initial configuration for the dynamic simulation of the ribbon-on-ribbon system. b) The ribbon lifts up the side with more intercalated water to let it escape from the interface; c) The layers collide under the combined effect of the vertical load and the lateral shear. The red circle highlights the replacement of a S atom by a water molecule, which may be the initial step for the oxidation of the MoS_2 layer.

We found no tendency of the edges towards sliding against each other, confirming that sliding actually takes place between the layers and not at grain boundaries.[2] Moreover, although in this case only one water molecule out of four undergoes OH/H dissociation (an outcome supported by the relatively small 0.6 eV energy gain for a dissociative H/OH adsorption over the molecular H_2O one, as shown in Figure 5), it confirms the active role of edges in removing water from the interface.

Finally, we note that one of the water molecules adsorbed on the edges (highlighted by a red circle in Figure 6c) dissociates into OH and H in the following steps of the dynamics; however, no further evolution of the edge structure is evidenced. Water therefore seems able to coordinate exposed Mo atoms on the edges but not to catalyse a major and rapid degradation of the MoS_2 layer in the simulated time interval. An additional dynamic run provided almost identical results: this further suggests that even in the presence of modifications of the regular stoichiometry of the layer, the overall MoS_2 sliding process is markedly influenced by the intercalated water molecules even when no oxidation mechanisms are active yet. As a multiple-step process probably requiring significant degrees of edge disruptions, oxidation would take place on a longer timescale even at the high contact pressures modelled here. The timescale of our simulations nevertheless allows us to show that water physisorption can impede the sliding motion in MoS_2 even in the absence of any oxidation. The latter has been shown to be favoured in the presence of molecular oxygen and high-temperature conditions.

4. Conclusions

Based on ab initio molecular dynamics calculations, we modelled the interaction of water with MoS_2 bilayers, both on basal planes and on the edges. The main outcomes may be summarised as: (1) The sliding distance and velocity are reduced by increasing amounts of water molecules at the interface following a viscous friction behaviour. (2) Simple S-vacancies on the basal plane do not affect the sliding properties and do not catalyse chemical reactions. (3) When possible, water diffuses away from the interface aided by the load and the presence of edges. (4) Both molecular and dissociative adsorption of water was observed on armchair edges, but no major signs of oxidation are evidenced in the simulated time intervals. (5) MoS_2 ribbons tend to slide along the basal planes after water removal rather than along grain boundaries.

Together, the evidence points to the conclusion that, at ordinary temperatures and in the absence of molecular oxygen, the main mechanism behind the decrease of lubricating performance of MoS_2 in humid environments is the physical interaction of molecular water with the layers. Despite being only mildly physisorbed on the basal plane and keeping the layers at a larger distance, water molecules are therefore able to effectively disrupt the sliding motion. Indeed, when mechanisms of water removal from the interface are active—such as the presence of edges—MoS_2 layers tend to regain their intercalant-free, layered stacking, which is the prerequisite for ultralow friction. This points to the fact that the interlayer region in MoS_2 is hydrophobic despite the weak hydrophilic character of the isolated layer.

Our results, which support initial experimental evidence along the same direction,[27,28] may help in the search for effective means to retain the extraordinary lubricant properties of MoS_2 also in the presence of water. Indeed, the results provide microscopic evidence for the detrimental role of the physical interactions between the sliding layers and the intercalated molecules. Our simulations reveal that, at ordinary temperatures in anaerobic conditions, water can increase MoS_2 friction even in the absence of any chemical oxidation. This suggests the possibility of conceiving and fabricating nano-interfaces with apertures or dopants,[34,58] or of tuning the applied load to remove water from the interface.

Acknowledgements

This work was partially supported by the University of Modena and Reggio Emilia through the FAR project "Understanding tribological phenomena in solid lubricants". Computer resources were provided by the CINECA Supercomputing Center through Grant ISCRA "water-TMD.

Keywords: materials science · mechanical properties · physisorption · solid-state structures · surface analysis

[1] X. Li, H. Zhu, *J. Materiomics* **2015**, *1*, 33 – 44.
[2] W. O. Winer, *Wear* **1967**, *10*, 422 – 452.
[3] J. M. Martin, C. Donnet, T. Le Mogne, T. Epicier, *Phys. Rev. B* **1993**, *48*, 10583 – 10588.
[4] T. W. Scharf, S. V. Prasad, *J. Mater. Sci.* **2013**, *48*, 511 – 531.
[5] C. Lee, Q. Li, W. Kalb, X.-Z. Liu, H. Berger, R. W. Carpick, J. Hone, *Science* **2010**, *328*, 76 – 80.
[6] C. Donnet, J. M. Martin, T. Le Mogne, M. Belin, *Tribol. Int.* **1996**, *29*, 123 – 128.
[7] W. Z. Teo, E. L. K. Chng, Z. Sofer, M. Pumera, *Chem. Eur. J.* **2014**, *20*, 9627 – 9632.
[8] E. L. K. Chng, M. Pumera, *RSC Adv.* **2015**, *5*, 3074 – 3080.
[9] J. K. G. Panitz, L. E. Pope, J. E. Lyons, D. J. Staley, *J. Vac. Sci. Technol. A* **1988**, *6*, 1166 – 1170.
[10] M. Chhowalla, G. A. J. Amaratunga, *Nature* **2000**, *407*, 164 – 167.
[11] X. Zhao, S. S. Perry, *ACS Appl. Mater. Interfaces* **2010**, *2*, 1444 – 1448.
[12] M. Tagawa, K. Yokota, K. Matsumoto, M. Suzuki, Y. Teraoka, A. Kitamura, M. Belin, J. Fontaine, J. M. Martin, *Surf. Coat. Technol.* **2007**, *202*, 1003 – 1010.
[13] G. J. Dudder, X. Zhao, B. Krick, W. G. Sawyer, S. S. Perry, *Tribol. Lett.* **2011**, *42*, 203 – 213.
[14] T. Polcar, A. Cavaleiro, *Surf. Coat. Technol.* **2011**, *206*, 686 – 695.
[15] X.-Z. Ding, X. T. Zeng, X. Y. He, Z. Chen, *Surf. Coat. Technol.* **2010**, *205*, 224 – 231.
[16] A. P. S. Gaur, S. Sahoo, M. Ahmadi, S. P. Dash, M. J.-F. Guinel, R. S. Katiyar, *Nano Lett.* **2014**, *14*, 4314 – 4321.
[17] X.-R. Shi, S.-G. Wang, J. Hu, H. Wang, Y.-Y. Chen, Z. Qin, J. Wang, *Appl. Catal. A* **2009**, *365*, 62 – 70.
[18] K. K. Ghuman, S. Yadav, C. V. Singh, *J. Phys. Chem. C* **2015**, *119*, 6518 – 6529.
[19] C. Ataca, S. Ciraci, *Phys. Rev. B* **2012**, *85*, 195410.
[20] B. Luan, R. Zhou, *Appl. Phys. Lett.* **2016**, *108*, 131601 – 131605.
[21] Q. Li, J. Song, F. Besenbacher, M. Dong, *Acc. Chem. Res.* **2015**, *48*, 119 – 1127.
[22] G. Levita, P. Restuccia, M. C. Righi, *Carbon* **2016**, *107*, 878.
[23] J. Zhang, T. Wang, P. Liu, S. Liu, R. Dong, X. Zhuang, M. Chen, X. Feng, *Energy Environ. Sci.* **2016**, *9*, 2789 – 2793.
[24] T. Liang, W. G. Sawyer, S. S. Perry, S. B. Sinnott, S. R. Phillpot, *Phys. Rev. B* **2008**, *77*, 104105.
[25] T. Liang, W. G. Sawyer, S. S. Perry, S. B. Sinnott, S. R. Phillpot, *J. Phys. Chem. C* **2011**, *115*, 10606 – 10616.
[26] B. C. Windom, W. G. Sawyer, D. W. Hahn, *Tribol. Lett.* **2011**, *42*, 301 – 310.
[27] H. S. Khare, D. L. Burris, *Tribol. Lett.* **2014**, *53*, 329 – 336.
[28] H. S. Khare, D. L. Burris, *Tribol. Lett.* **2013**, *52*, 485 – 493.
[29] B. Radisavljevic, A. Radenovic, J. Brivio, V. Giacometti, A. Kis, *Nat. Nanotechnol.* **2011**, *6*, 147 – 150.
[30] M. Chhowalla, H. S. Shin, G. Eda, L.-J. Li, K. P. Loh, H. Zhang, *Nat. Chem.* **2013**, *5*, 263 – 275.
[31] J. He, K. Hummer, C. Franchini, *Phys. Rev. B* **2014**, *89*, 075409.
[32] H. Qiu, L. Pan, Z. Yao, J. Li, Y. Shi, X. Wang, *Appl. Phys. Lett.* **2012**, *100*, 123104.
[33] D. J. Late, B. Liu, H. S. S. R. Matte, V. P. Dravid, C. N. R. Rao, *ACS Nano* **2012**, *6*, 5635 – 5641.
[34] C. Ataca, S. Ciraci, *J. Phys. Chem. C* **2011**, *115*, 13303 – 13311.
[35] D. D. Fan, H. J. Liu, L. Cheng, P. H. Jiang, J. Shi, X. F. Tang, *Appl. Phys. Lett.* **2014**, *105*, 133113.
[36] K. Dolui, C. D. Pemmaraju, S. Sanvito, *ACS Nano* **2012**, *6*, 4823 – 4834.
[37] A. Blumberg, U. Keshet, I. Zaltsman, O. Hod, *J. Phys. Chem. Lett.* **2012**, *3*, 1936 – 1940.
[38] C. Ataca, H. Sahin, E. Akturk, S. Ciraci, *J. Phys. Chem. C* **2011**, *115*, 3934 – 3941.
[39] L. P. Hansen, Q. M. Ramasse, C. Kisielowski, M. Brorson, E. Johnson, H. Topse, S. Helveg, *Angew. Chem. Int. Ed.* **2011**, *50*, 10153 – 10156; *Angew. Chem.* **2011**, *123*, 10335 – 10338.
[40] G. Zilibotti, S. Corni, M. C. Righi, *Phys. Rev. Lett.* **2013**, *111*, 146101.
[41] R. Car, M. Parrinello, *Phys. Rev. Lett.* **1985**, *55*, 2471 – 2474.
[42] P. Giannozzi, S. Baroni, N. Bonini, M. Calandra, R. Car, C. Cavazzoni, D. Ceresoli, G. L. Chiarotti, M. Cococcioni, I. Dabo, A. Dal Corso, S. de Gironcoli, S. Fabris, G. Fratesi, R. Gebauer, U. Gerstmann, C. Gougoussis, A. Kokalj, M. Lazzeri, L. Martin-Samos, N. Marzari, F. Mauri, R. Mazzarello, S. Paolini, A. Pasquarello, L. Paulatto, C. Sbraccia, S. Scandolo, G. Sclauzero, A. P. Seitsonen, A. Smogunov, P. Umari, R. M. Wentzcovitch, *J. Phys. Condens. Matter* **2009**, *21*, 395502; http://www.quantum-espresso.org.
[43] S. Kajita, M. C. Righi, *Carbon* **2016**, *103*, 193 – 199.
[44] M. V. Bollinger, J. V. Lauritsen, K. W. Jacobsen, J. K. Nørskov, S. Helveg, F. Besenbacher, *Phys. Rev. Lett.* **2001**, *87*, 196803.
[45] Y. Li, Z. Zhou, S. Zhang, Z. Chen, *J. Am. Chem. Soc.* **2008**, *130*, 16739 – 16744.
[46] S. Grimme, *J. Comput. Chem.* **2006**, *27*, 1787 – 1799.
[47] T. Bucko, J. Hafner, S. Lebègue, J. G. Ángyán, *J. Phys. Chem. A* **2010**, *114*, 11814 – 11824.
[48] J. P. Perdew, K. Burke, M. Ernzerhof, *Phys. Rev. Lett.* **1996**, *77*, 3865 – 3868.
[49] D. Vanderbilt, *Phys. Rev. B* **1990**, *41*, 7892 – 7895.
[50] T. Björkman, A. Gulans, A. V. Krasheninnikov, R. M. Nieminen, *Phys. Rev. Lett.* **2012**, *108*, 235502.
[51] G. Levita, A. Cavaleiro, E. Molinari, T. Polcar, M. C. Righi, *J. Phys. Chem. C* **2014**, *118*, 13809 – 13816.
[52] G. Levita, E. Molinari, T. Polcar, M. C. Righi, *Phys. Rev. B* **2015**, *92*, 085434.
[53] M. Methfessel, A. T. Paxton, *Phys. Rev. B* **1989**, *40*, 3616 – 3621.
[54] G. Cicero, A. Calzolari, S. Corni, A. Catellani, *J. Phys. Chem. Lett.* **2011**, *2*, 2582 – 2586.
[55] W. Zhou, X. Zou, S. Najmaei, Z. Liu, Y. Shi, J. Kong, J. Lou, P. M. Ajayan, B. I. Yakobson, J.-C. Idrobo, *Nano Lett.* **2013**, *13*, 2615 – 2622.
[56] J. A. Spirko, M. L. Neiman, A. M. Oelker, K. Klier, *Surf. Sci.* **2003**, *542*, 192 – 204.
[57] J. Hong, Z. Hu, M. Probert, K. Li, D. Lv, X. Yang, L. Gu, N. Mao, Q. Feng, L. Xie, J. Zhang, D. Wu, Z. Zhang, C. Jin, W. Ji, X. Zhang, J. Yuan, Z. Zhang, *Nat. Commun.* **2015**, *6*, 6293.
[58] H.-P. Komsa, J. Kotakoski, S. Kurasch, O. Lehtinen, U. Kaiser, A. V. Krasheninnikov, *Phys. Rev. Lett.* **2012**, *109*, 035503.

Manuscript received: October 19, 2016
Revised manuscript received: December 5, 2016
Accepted manuscript online: December 5, 2016
Version of record online: January 9, 2017